A spectroscopic study of uranyl speciation in chloride-bearing solutions at temperatures up to 250 $^{\circ}\text{C}$

A.A. Migdisov ^{1*}, H. Boukhalfa ¹, A. Timofeev ², W. Runde ¹, R. Roback ¹, and A.E. Williams-Jones ²

¹Los Alamos National Laboratory, P.O. Box 1663, M.S. J535, Los Alamos, NM 87545, US

²Department of Earth and Planetary Sciences, McGill University, 3450 University Street, Montreal, Canada, H3A 0E8

1 *corresponding author: artas@lanl.gov

Abstract

3

The speciation of U in NaCl-bearing solutions at temperatures up to 250 °C and concentrations 4 of NaCl up to 1.5 m has been investigated using an in situ spectroscopic technique. The recorded 5 spectra permit us to identify the species present in the solutions as UO₂²⁺, UO₂Cl⁺, and UO₂Cl₂°. 6 7 UO₂Cl₃⁻ is also likely present at high temperatures and NaCl concentrations, but concentrations of this species are insufficient for derivation of the formation constants. No evidence was found 8 for species of higher ligand (Cl⁻) number. Thermodynamic stability constants derived for these 9 species show fair agreement with published data for 25 °C, but differ significantly from those 10 predicted by an earlier high-temperature study (Dargent et al., 2013), which suggested that 11 UO₂Cl₄²- and UO₂Cl₅³- contribute significantly to the mass balance of uranyl chloride complexes, 12 especially at high temperature. In contrast, our data suggest that the main uranyl-chloride 13 complex present in aqueous solutions at T > 150 °C and concentrations of NaCl relevant to 14 natural hydrothermal systems is UO₂Cl₂°. The values of the logarithms of thermodynamic 15 formation constants (β) for the reaction $UO_2^{2+} + Cl^- = UO_2Cl^+$ are 0.02, 0.25, 0.55, 1.09, 1.59, 16 and 2.28 derived at 25, 50, 100, 150, 200, and 250 °C, respectively. For the reaction UO_2^{2+} + 17 $2Cl^{2} = UO_{2}Cl_{2}^{\circ}$ the values of log β derived at these temperatures are 0.4, 0.58, 0.74, 1.44, 2.18, 18 and 3.42. Values of the formation constant estimated for uranyl-chloride species predict the high 19 concentrations of U observed by Richard et al. (2011) in fluid inclusions of the giant McArthur 20 River unconformity-type uranium deposit. 21

1. Introduction

23

24

25

26

27

28

29

30

31

32

33

34

35

36

37

38

39

40

41

42

43

44

45

A large proportion of uranium deposits, including the giant Olympic Dam deposit in Australia and the giant McArthur River unconformity-type uranium deposit in Canada have been shown to have formed through hydrothermal scavenging, transport and deposition of uranium (e.g., Oreskes and Einaudi, 1992; Richard et al., 2011). Understanding of the factors governing the behavior of uranium in aqueous solutions at elevated temperatures is therefore crucial for predicting the conditions favorable for uranium ore formation and, in turn, developing robust, quantitative models for the genesis of these deposits. In addition to evaluating uranium ore-forming processes, accurate assessment of the hydrothermal mobility of uranium is also essential for understanding risks associated with nuclear accidents and the disposal of nuclear waste in geological formations (e.g., Burns et al., 2012; Ewing, 2015). In naturally occurring hydrothermal systems, including those responsible for uranium ore formation, one of the most common ligands is chloride, which typically is present in hydrothermal ore-forming fluids at concentrations exceeding 10 wt% NaCl equiv. For example, Oreskes and Einaudi (1992) reported concentrations of NaCl in fluid inclusions from the Olympic Dam deposit of up to 42 wt % NaCl equiv. The data collected for the giant McArthur River deposit also suggest the involvement of extremely saline brines containing up to 52 wt% NaCl (equivalent to 9 m [mol/kg]) (Derome et al., 2005). Further support for an association of high salinity brines and uranium deposits, is also provided by the comprehensive review of Cuney (2009) who cited numerous studies reporting high concentrations of NaCl in fluid inclusions from a variety of types of uranium deposits. Thus, despite the fact that aqueous chloride complexes of uranium are generally considered weak (Guillaumont et al., 2003), the very high concentration of chloride in these fluids can potentially overcome this weakness and make uranylchloride complexes important agents for the mobilization and transport of uranium in ore-forming

systems. This is the case for the hydrothermal transport of the rare earth elements (REE), for which we have demonstrated that weak chloride complexes can compete successfully with other species due to the very high concentrations of chloride typical in ore forming fluids (Migdisov et al., 2016). Experimental studies, employing spectroscopic, chromatographic, electromotive force, and highenergy X-ray scattering techniques at ambient temperature (Ahrland, 1951; Davies and Monk, 1957; Choppin and Du, 1992; Runde et al., 1996; Soderholm et al., 2011), have documented the existence of UO₂Cl⁺, UO₂Cl₂°, and UO₂Cl₃⁻ in aqueous solutions, and have determined their thermodynamic stability constants. The data available for elevated temperature, however, are limited to a single study, namely that of Dargent et al. (2013), which employed in situ hightemperature Raman spectroscopy up to 350 °C. In addition to the species determined at low temperature, Dargent et al. (2013) also identified species of significantly higher chloride/U ratios, i.e., UO₂Cl₄²- and UO₂Cl₅³-. Surprisingly, the species distribution predicted by the thermodynamic stability constants obtained in this study, attributed an appreciable contribution of these high ligand number species to the mass balance of uranyl-chloride complexes in saline solution at T>150 °C. . As discussed in Seward et al., (2014), increasing temperature generally leads to the destabilization of highly charged species and a larger contribution of neutral and weakly charged complexes because of the changing properties of water with increasing temperature. Without questioning quality of the spectral data collected by Dargent et al. (2013), we suspect that their derivation of the formation constants for UO₂Cl₄²⁻ and UO₂Cl₅³⁻ can be associated with uncertainties significantly larger than those reported in the paper. As their experiments were performed with LiCl solutions having a molarity of up to 3 M [mol/dm³] (12 M for peaks identification), accurate derivation of the thermodynamic stability constants would require application of a Pitzer-based activity model (e.g., Pitzer and Silvester, 1978; Monnin, 1990; Anderko and Pitzer, 1991).

46

47

48

49

50

51

52

53

54

55

56

57

58

59

60

61

62

63

64

65

66

67

However, as the parameters for such a model are not available for the temperatures investigated by Dargent et al. (2013), they were forced to use the much simpler model of Helgeson et al. (1981) (which was developed mostly for NaCl-based solutions), and, based on specific-ion theory (Grenthe et al., 1992), to correct for the deviations from this model that would make it applicable to LiCl. Such corrections can potentially introduce considerable error, and may lead to sizable shifts in the values of the derived stability constants from their true values. On another hand, it has recently been demonstrated that under some circumstances co-ordination/entropy-driven processes can stabilize highly charged complexes at elevated temperatures (Brugger et al., 2016), and this potentially might be the case of uranyl-chloride speciation. All the above suggests that the findings of Dargent et al. (2013) require verification, preferably performed by independent experimental technique. The goals of our study therefore are: 1) to investigate the stability of uranyl-chloride species at elevated temperature using an experimental technique different from that used before; and 2) to design the study in a way that would enable us to avoid potential problems associated with an unproven activity model. This study is based on electronic spectra of uranyl chloride solutions, collected in situ at temperatures up to 250 °C. As the most reliable and experimentally best-tuned activity model applicable to high temperature is that developed by Helgeson et al. (1981), Oelkers and Helgeson (1990) and Oelkers and Helgeson (1991) for NaCl-dominated solutions (recommended for up to I = 6 and T up to $600 \,^{\circ}$ C), we employed NaCl-based solutions, rather than the LiCl-based solutions used by Dargent et al. (2013). Moreover, in order to optimize the reliability of the above model, we restricted concentrations of NaCl in our experimental solutions to 1.5 M.

69

70

71

72

73

74

75

76

77

78

79

80

81

82

83

84

85

86

87

88

89

2. Experimental technique

91

92

93

94

95

96

97

98

99

100

101

102

103

104

105

106

107

108

109

110

111

112

113

The experiments involved recording isothermal sets of spectra for solutions having a systematically changing ratio of uranyl and chloride concentration. Spectra were recorded over the wavelength range of 350 to 700 nm in increments of 0.2 nm using a Cary 5000 spectrophotometer. This range of wavelengths was selected to quantify the shifts associated with the ligand-metal charge transfer absorbance of uranyl species at 350-500 nm (Runde, 2000; Hagberg et al., 2005; Ruipérez and Wahlgren, 2010; Sun et al., 2015), and, at the same time, to be able to identify the potential reduction of uranyl to U(IV) species, which should be manifested by increasing absorbance at 600-650 nm (Runde, 2000; Tutschku et al., 2004; Nagai et al., 2005). The records demonstrating absorbance increase at this wavelength range were excluded and further spectral treatment was performed only for the 350-550 nm wavelength range. Isothermal measurements were made at 25, 50, 100, 150, 200, and 250 °C and a pressure of 100 bar using a high-temperature, flow-through spectroscopic cell built from grade 2 titanium, and equipped with two sapphire windows based on the design proposed in Suleimenov (2004) (Figure 1). Prior to the experiments, the cell surfaces were passivated to ensure chemical inertness of the vessel by heating at 400 °C in air for 12 hours, which resulted in the formation of thin and dense layers of TiO₂. Sapphire windows were sealed into the cell body using gold o-rings and retainers. The experimental solutions were pumped into the cell through titanium and PEEK capillaries using a PEEK HPLC pump; pressure was maintained at 100 ± 1 bar using a PEEK back pressure regulator. The cell was heated to the temperature of interest using four cartridge heaters; temperature was maintained within ±0.1° C using an Omega CSi32 temperature controller. The 25 °C path length of the cell (0.85 cm) was determined by comparing the absorbance at 414 nm of uranyl solutions (UO₃ dissolved in triflic acid, Trifluoromethanesulfonic acid, CF₃SO₃H, Acros Organics, 99%, extra

path length with temperature were minor, but were accounted for using the value of the thermal expansion of Ti $(8.6 \cdot 10^{-6} \text{ m/(m K)})$. Considering that CO₂ is present in the atmosphere, and is a strong binding ligand for uranyl-ions (Guillaumont et al., 2003), the uranyl stocks were prepared by dissolving UO₃ solid (99.8% International Bio-Analytical Industries, Inc.) in degassed CO₂-free distilled water with large excess of triflic acid to maintain the pH of the stock in the range of 0.8 - 1.1; triflic acid was selected because it is a non-complexing ligand able to withstand high temperatures (Bergstrom and J., 1990; Greenwood and A., 1992; Wood et al., 2002). After dissolution, the stock solution was flushed intensively with Ar to remove any traces of CO₂. Uranium concentrations in stock solution were determined in diluted samples by ICP-MS, and were typically in the range of 21 to 25 mM. Although highly acidic and, thus, unable to dissolve significant concentrations of CO₂, fresh uranyl stocks were made for each experiment in order to avoid undue exposure to the atmosphere. Experimental solutions were prepared by diluting the stock with degassed CO₂-free NaCl solutions (ACS, Fisher Scientific); solutions were prepared so as to have the same initial concentration of uranyl ions and variable concentrations of NaCl. Experimental solutions comprise sets with concentrations of 4, 7, 9, and 12 mM (25 °C) of total uranyl-ion (the series having 4 mM was abandoned for experiments at T <150 °C due to the low absorbance); the concentrations of NaCl for each series ranged from 0.01 to 0.7-1.5 M (25 °C); the pH_{25°C} of the experimental solutions was set at 1.5-1.8 by acidifying the uranyl stock solution with triflic acid. In order to interpret the molar absorbances of the simple hydrated uranyl-ion, each of the above series involved an initial chloride-free solution, which was obtained by dilution of the uranyl stock with degassed CO₂-free

pure) recorded in the cell and in a standard quartz cuvette with 1.0 cm path length; changes of the

114

115

116

117

118

119

120

121

122

123

124

125

126

127

128

129

130

131

132

133

134

distilled water. The full list of the compositions of the solutions investigated in this study is reported in the Electronic Annex to this paper.

In order to ensure that the recorded spectra represent a state of equilibrium, test spectra were collected for selected solutions at flow rates ranging from 0.05 to 0.3 ml/min, which provided for complete exchange of the solutions in the cell in 20 to 3 minutes, respectively. No changes in the spectra were detected during these runs, suggesting that equilibrium was established in less than 3 minutes after the solution entered the heated cell. The spectra collected at higher flow rates were however characterized by higher spectral noise and poorer quality of temperature control. Isothermal absorbance spectra were therefore collected at flow rates of 0.05-0.01 ml/min. Replacement of the solutions in the cell was performed by flushing the cell with a new solution at a flow rate of 2.5 ml/min for duration of 10 minutes. In order to account for the absorbance of the sapphire windows (baseline correction), the absorbance spectra of nanopure water were recorded at the beginning and end of each of the recording cycles. All of the spectra presented in this paper are background-corrected; the uncertainties of measurement (±0.002 absorbance units) were estimated based on repeated scans of the same solutions.

3. Results

The spectra collected in our study for triflic acid-based chloride-free solutions were used to obtain molar absorbance spectra (molar extinction coefficients) for the hydrated UO_2^{2+} ion. These spectra are illustrated in Figure 2; the values of the derived molar absorbances are reported in the Electronic Annex to this paper (please note that the values reported there are the results of raw spectral fitting and are therefore for the path length of the cell such as $l_{25} \circ c = 0.85$ cm).

Figure 3 illustrates the spectral effect associated with adding NaCl to solutions containing 7.1 mM of total uranyl-ion. The spectra shown in this Figure have been background-corrected and normalized assuming zero absorbance of a background-corrected spectrum at 700 nm. The spectra in Figure 3 show that an increase of chloride concentration leads to an increase in band intensity and a red shift of the absorbance peak. Increasing temperature increases this effect. Both a temperature increase and an increasing chloride concentration contribute to the expansion of the shoulder of the UV peak, and we speculate that expansion of its shoulder may contribute appreciably to the increase of the absorbance intensity at 370-550 nm. These effects are most likely associated with absorbance of species other than UO₂²⁺, namely, uranyl chloride complexes. Figure 4 illustrates the changes in absorbance recorded for solutions containing 7.1 mM of total uranyl-ion at selected wavelengths as a function of NaCl concentration. These spectra show that absorbances increase steadily and systematically with increasing of chloride concentration. The only exceptions are the spectra collected at low temperature (25 and 50 °C): the changes of the absorbance values observed at 414 nm are extremely small, and, moreover, the absorbance likely decreases at the highest concentration of NaCl, indicating formation of an isosbestic point. It should be noted however that the amplitude of changes recorded for 25 and 50 °C at 414 nm does not exceed 0.003-0.004 absorbance units. This is very close to the uncertainty of the spectral recording (tolerance = 0.002), and therefore can potentially be an artifact of a systematically changing background absorbance of the cell. Nevertheless, when plotted as a function of the logarithm of NaCl concentrations (Figure 4c and 4d), in most of the cases, the absorbance values show a clear linear dependence at low and moderate concentrations of NaCl, suggesting an appreciable concentration of at least one uranyl-chloride species in the aqueous solution. The deviation from linearity observed at higher concentrations of NaCl can be explained by a variety

157

158

159

160

161

162

163

164

165

166

167

168

169

170

171

172

173

174

175

176

177

178

of different contributing factors, such as the presence of another uranyl-chloride complex, the influence of changing activity of the solution components, or a decrease in the activity of free chloride-ions due to increasing ion pairing of NaCl. Quantitative interpretation of the collected spectra therefore requires numerical quantitative modeling.

4.0.3.1. Spectral treatment

4.1.0.3.1.1. Speciation model

Each isothermal set of spectra collected in our experiments is represented as an absorbance matrix A(k,j), in which each k (row) corresponds to a solution with a specific uranyl/chloride ratio, and each j (column) corresponds to a wavelength at which the absorbance was recorded. We assumed that the spectra obey the Lambert-Beer law:

$$190 \quad \frac{A}{L} = \sum_{i=1}^{n} \varepsilon_i M_i \tag{1}$$

where A is the measured absorbance at a given wavelength, L is the path length, ε_i is the molar absorbance of the ith species, and M_i is the molar concentration of the species i. Based on this assumption, the number of absorbing species that form the matrix A(k,j) is equal to the number of linearly independent vectors in the matrix. The latter is the rank of the matrix A(k,j) and therefore, in order to determine the number of the absorbing species, we calculated the rank of the matrix A(k,j) for the experimentally determined tolerance (Suleimenov and Seward, 1997; Migdisov and Williams-Jones, 2006; Migdisov et al., 2008; Liu et al., 2012). The results of this analysis are shown in Figure 5(a-c) from which it is evident that the number of absorbing species varies between 3 and 4. The contribution of the fourth absorbing species is small, and only can be detected if the spectral accuracy is better than 0.0037 at 25 °C and 0.0073 at 250 °C. These values are only

~2 to 3.5 times greater than the experimentally determined accuracy of the spectral recording (0.002), and we therefore conclude that, although we are able to detect a contribution from the fourth absorbing species to the spectra, any derivation of the properties of this species will likely be associated with an unacceptably high uncertainty. Moreover, the contribution of the above species to the spectral picture can be detected at only the highest concentrations of NaCl used in our experiments. Reduction of the absorbance matrix to m(NaCl) ≤ 1 M, and $\lambda \geq 360$ nm results in decrease of the number of absorbing species to 3 (Figure 5,d-f). Our following derivations were therefore performed for the reduced absorbance matrix, assuming that it is defined by three absorbing species. The probable absorbing species were identified from published data. Considering that the solutions employed in our experiments had a pH_{25°C} in the range of 1.2 to 1.5, uranyl-hydroxyl species were not included in our speciation model (Grenthe et al., 1992; Guillaumont et al., 2003). We also excluded uranyl carbonate complexes because of the precautions taken to ensure the carbonatefree nature of experimental solutions and the low solubility of CO2 in highly acidic solutions (Sander, 2006). Soderholm et al. (2011) identified the following uranyl species at 25 °C: UO₂Cl⁺, UO₂Cl₂°, and UO₂Cl₃⁻. The species UO₂Cl₃⁻ has been identified at concentrations of chloride significantly higher than 1.0 M, and we therefore suggest that this species will have a very minor contribution to the spectra as discussed above. Dargent et al. (2013) also identified these three species for temperatures up to 150 °C. Thus, the speciation model (that we used in our derivations for temperatures up to 150 °C involved UO₂²⁺, UO₂Cl⁺, and UO₂Cl₂° (reduced absorbance matrix, "the low charge model"). For higher temperatures, however, Dargent et al. (2013) observed UO₂Cl₃-, UO₂Cl₄²-, and UO₂Cl₅³- as the dominant species. For our derivations at temperatures above 100 °C, and in parallel with "the low charge model", we therefore also tested an alternative

201

202

203

204

205

206

207

208

209

210

211

212

213

214

215

216

217

218

219

220

221

222

model, in which uranyl-bearing aqueous species are represented by UO ₂ ²⁺ , UO ₂ Cl ₃ ⁻ , and UO ₂ Cl ₄ ²
⁻ ("high charge model"). Dargent et al. (2013) observed occurrence UO ₂ Cl ⁺ only at temperatures
below 200 °C, and UO_2Cl_2 ° was only detected at T < 250 °C. It should be noted however, that
their experiments were mostly performed with solutions having significantly higher concentrations
of chloride. Only one solution of six studied (0.3, 1, 3, 5, 8, and 12 M LiCl) had concentrations
within the range of those used in our study. We therefore do not exclude that the low-chlorinity
species of uranyl might be overlooked by Dargent et al. (2013) at elevated temperatures. In order
to evaluate speciation of uranyl-chloride species suggested by the values of the stability constants
reported by Dargent et al. (2013) for the concentration range employed in our experiments, we
have fitted these values to the Ryzhenko-Bryzgalin (MRB) (Ryzhenko et al., 1985) model and
used the extrapolated values of β_1 , β_2 , β_3 , β_4 , and β_5 to determine the predominant uranyl-chloride
species returned by the model of Dargent et al. (2013) for the conditions of our experiments (see
below). It was found that their model suggests UO2Cl ⁺ and UO2Cl5 ³⁻ as the main species
controlling uranyl mass balance in our experimental solutions at T>100 °C. In order to check this
hypothesis, we also tested the third alternative model ("mixed species model"), which involved
$UO_2^{2+}, UO_2Cl^+, and UO_2Cl_5, at$ temperatures of 150, 200, and 250 °C. ³
In addition to uranyl-bearing complexes, the speciation model also involves the non-absorbing
species: H ⁺ , Na ⁺ , Cl ⁻ , NaCl ^o , HCl ^o , and Tf(triflate). The thermodynamic data required for
modelling the solutions at each of the experimental temperatures were taken from Johnson et al.
(1992), Sverjensky et al. (1997), and Tagirov et al. (1997). As a non-complexing agent, triflate
contributes to the ionic strength and total molality of the solutions, but was assumed to not
participate in complex formation. The activities of the individual ions were calculated using the
extended Debye-Hückel model modified by Helgeson et al. (1981), Oelkers and Helgeson (1990)

and Oelkers and Helgeson (1991) for NaCl-dominated solutions (recommended for up to I=6 and T up to 600 °C):

$$\log \gamma_i = -\frac{AZ_i^2 \sqrt{I}}{1 + B\dot{a}\sqrt{I}} + b_{\gamma}I + \Gamma \tag{2}$$

where A and B are the Debye–Hückel solvent parameters, γ_i , Z_i and \dot{a}_i are the individual molal activity coefficient, the charge, and the distance of closest approach of an ion i, respectively. The effective ionic strength calculated using the molal scale is I, Γ is a molarity to molality conversion factor, and b_{γ} is the extended-term parameter for NaCl from Helgeson et al. (1981), Oelkers and Helgeson (1990) and Oelkers and Helgeson (1991).

4.2.0.3.1.2. Deconvolution of spectra and calculation of formation constants

- The deconvolution procedure used here is the same as that described in our previous studies (e.g., Migdisov et al., 2008; Migdisov and Williams-Jones, 2008; Migdisov et al., 2011; Liu et al., 2012). For details not provided in the following review, readers are referred to the above publications or to the paper of Brugger (2007), which discusses in detail the fitting algorithms and provides MATLAB-based codes for the derivation of formation constants from spectroscopic data.
- Formation constants for uranyl-chloride species are derived for the two models referred to above.
- The first, "low charge model" was tested for all temperatures and involved the following reactions
- 263 involving uranyl species:

250

251

252

253

254

255

256

257

258

259

264
$$UO_2^{2+} + Cl^- = UO_2Cl^+$$
 $\log \beta_1$ (3)

265
$$UO_2^{2+} + 2Cl^- = UO_2Cl_2^{\circ}$$
 $\log \beta_2$ (4)

The second, "high charge model", was tested for 150, 200, and 250 °C and involved the following reactions:

268
$$UO_2^{2+} + 3Cl^- = UO_2Cl_3^ \log \beta_3$$
 (5)

269
$$UO_2^{2+} + 4Cl^- = UO_2Cl_4^{2-}$$
 $\log \beta_4$ (6)

The third, "mixed species model", was tested for 150, 200, and 250 °C and involved the reaction

(3) and the reaction of formation of UO₂Cls³-

272 -

273
$$UO_2^{2+} + 5Cl^- = UO_2Cl_5^{3-}$$
 $\log \beta_5$ (7)

The fitting was performed iteratively for isothermal absorbance matrices. Arbitrary initial guesses were made for $\log \beta_1$ and $\log \beta_2$ (or $\log \beta_3$ and $\log \beta_4$ in the case of "high charge model"). In order to minimize the time of computation, we used the values reported by Dargent et al. (2013), or their extrapolations to higher temperatures as our initial guesses. Based on these initial guesses, the compositions of the experimental solutions, and the models discussed above, we calculated molal species distribution for each of the experimental solutions. The calculations were performed using a version of the EQBRM code (Anderson and Crerar, 1993) that has been rewritten in MATLAB (Liu et al., 2002; Brugger, 2007). The molal concentrations were converted to molar values (required by the Lambert-Beer law), based on the equation proposed for NaCl solutions by Bodnar (1983), taking into account the mass of dissolved components. These calculations provided the matrix of molar concentrations of absorbing aqueous species C. The following spectral deconvolution was based on a technique employing singular value decomposition (Golub and Reinsch, 1970) of the absorbance matrix A^{meas} developed for the deconvolution of infrared spectra

- by Hug and Sulzberger (1994) and subsequently applied to UV-Visible spectra by Boily and
- 288 Suleimenov (2006).
- 289 The singular value decomposition

290
$$[\mathbf{U}, \mathbf{S}, \mathbf{V}] = \text{SVD}(\mathbf{A}^{\text{meas}})$$
 (8)

- produces a diagonal matrix S of the same dimension as A^{meas} , with non-negative diagonal elements
- in decreasing order, and unitary matrices U and V so that

293
$$A^{\text{meas}} = \mathbf{U} \cdot \mathbf{S} \cdot \mathbf{V}'$$
 (9)

294 A substitute matrix **R** was calculated such that

$$\mathbf{R} = \mathbf{C}' \cdot \mathbf{U} \tag{10}$$

- 296 Considering equation (1) the matrix of molar absorbances, which provides the best approximation
- 297 to the guesses of formation constants used to calculate C, is therefore

$$\mathbf{E} = \mathbf{S} \cdot \mathbf{V}' / \mathbf{R} \tag{11}$$

299 A theoretical absorbance matrix based on the selected set of formation constants is:

$$300 A^{calc} = C \cdot E' (12)$$

- 301 The matrix A^{calc} averages the effects associated with changing metal/ligand ratios based on the
- selected initial guesses for the formation constants, and, in the general case, is significantly
- 303 different from A^{meas} .
- The following step involved calculation of the overall error, or, in other words, the misfit
- of the matrix A^{calc} to the matrix A^{meas} :

306
$$U = \sum_{i=1}^{I} \left[\sum_{j=1}^{J} \left(\frac{A_{ij}^{meas} - A_{ij}^{calc}}{A_{ij}^{meas}} \right)^{2} \right]$$
 (13)

where A_{ij}^{meas} and A_{ij}^{calc} are the measured and calculated absorbance at wavelength i for solution j. The value of the overall error (misfit) was iteratively minimized by changing the values of the formation constants using the algorithm of simplex minimization reported in Nelder and Mead (1965) and incorporated into the MATLAB functions library. An example of the improvement of the goodness of the fit after this minimization is illustrated on Figure 6. The set of formation constants corresponding to the minimal value of U was therefore selected as the best fit to the recorded spectra. The value of U was also used to select between "the low charge model", "the mixed species model" and "the high charge model": the model returning the lower value of U was selected as providing the best fit to the spectral data.

As discussed in (4.1), simultaneous derivation of several formation constants from spectroscopic data returns values associated with different uncertainty. The method by which the uncertainty was determined is described in detail in our earlier publications (e.g., Migdisov et al., 2006; Migdisov and Williams-Jones, 2006; Migdisov et al., 2008) and involves evaluating the effect on the profile of U with changes in the guesses of the values for the formation constants. The range of values for a formation constant for which the overall error is lower than the accuracy of the measurement gives the uncertainty associated with its derivation. An example of such a profile is shown on Figure 7.

4.3.3.2. Results of the treatment of the spectra

The overall misfit of "the low charge model", "the mixed species model" and "the high charge model" to the spectra recorded at 150, 200, and 250 °C is reported in Table 1. As can be seen from

this table, the misfits of both "the high charge model" and "the mixed species model" are significantly greater at all temperatures than the misfit associated with "the low charge model"; the difference between these values varies from a half to two orders of magnitude at 150 and 250 °C, respectively. We therefore conclude that, for the concentration range employed in our experiments, there is not a significant contribution of highly charged uranyl-chloride complexes to the mass balance of these species. Accordingly, we abandoned "the high charge model" and "the mixed species model". Nevertheless, we do not exclude the possibility that species with a ligand number (Cl⁻) greater than that of UO₂Cl₂° may became spectroscopically visible at concentrations of NaCl higher than those employed in our study. Spectroscopic properties of the uranyl-ion have been investigated intensively since the late 1940s (e.g., Dieke and Duncan, 1949; Rabinovitch and Belford, 1964). Meinrath (1998) described the electronic structure of UO_2^{2+} as occupied molecular orbitals with mostly O-2p σ_u -HOMO bonds. The LUMO orbital is formed by an empty $5f_{\phi}$ orbital. The characteristic low-lying electronic transition takes place from the ground state σ_u -MO to the non-bonding f orbitals. The spectra of UO₂²⁺ reported in the literature display an absorption band in the range 480 nm and 330 nm with a characteristic fine structure, resulting from coupling of electronic transitions with symmetric stretching vibrations of the uranyl(VI) group (Jones, 1958; De Jagere and Görller-Walrand, 1969), and a nearly continuous spectrum beyond 330 nm without characteristic features. The absorbance maximum is at 413.8 nm and has a molar extinction coefficient of 9.7 ± 0.2 dm³ mol⁻¹ cm⁻¹ (Meinrath, 1997; Meinrath, 1998). Our data collected at 25 °C for UO₂²⁺ closely reproduce the values reported in the literature: the maximum molar absorbance detected for the band at 370-550 nm was at 414.8 nm with an extinction coefficient of 9.9 dm³ mol⁻¹ cm⁻¹ (8.42 dm³ mol⁻¹ cm⁻¹ derived for 0.85 cm path length).

327

328

329

330

331

332

333

334

335

336

337

338

339

340

341

342

343

344

345

346

347

348

The spectra in Figure 2, show a gradual increase in the intensity of the absorbance, a broadening of the peak, and its gradual, but minor, shift to lower energy (red shift) with increasing temperature. Similar effects have been reported by Suleimenov et al. (2007) for temperatures up to 150 °C for the molar absorbance of uranyl ions in nitrate-based solutions. It should be noted, however, that the values reported by Suleimenov et al. (2007) are \sim 5% lower than those obtained in our study. In addition, temperature increases lead to significant expansion of the band located beyond 330 nm. It is also worth noting that a similar expansion of the high energy band with increasing temperature has been documented in a number of previous spectroscopic studies performed at T > 25 °C (e.g., Zanonato et al., 2004; Suleimenov et al., 2007).

Smoothed molar absorbances derived for UO₂Cl⁺ and UO₂Cl₂°, are illustrated in Figure 8. For most of the solutions investigated, the contribution of UO₂Cl⁺ to the recorded spectra was found to be the highest for the uranyl species considered here and the corresponding molar absorbance was also the most reliably determined. The contribution of UO₂Cl₂° was lower, although it increased with increasing temperature; molar absorbances determined for this species are mostly associated with higher uncertainty than those for UO₂Cl⁺. In this study, we did not evaluate the uncertainty associated with each of the determined molar absorbances because of technical difficulties associated with determining these values for the wavelength range 350-500 nm and a 0.2 nm increment. The uncertainty, however, was accounted for in evaluating the errors associated with derivation of each of the formation constants; the latter values provide some indication of the reliability of the derived molar absorbances. From Figure 8, it is evident that the values of the derived molar absorbances increase with increasing temperature and undergo a minor, but systematic, red shift. A similar effect was observed for increasing chlorination number, i.e., increases with the number of chloride ions bound to the uranyl ion is accompanied by a shift to

lower energy (Figure 9). The values of the thermodynamic formation constants derived for the Reactions 3 and 4 together with the uncertainty associated with each of these values are listed in Table 2.

5.4. Discussion

373

374

375

376

377

378

379

380

381

382

383

384

385

386

387

388

389

390

391

392

393

394

395

Table 3 compares the values of the formation constants determined at 25 °C for UO₂Cl⁺ and UO₂Cl₂°, (log β₁ and log β₂, Reactions 3 and 4) obtained in this study with those reported in the literature. As can be seen from this Table, our data suggest that the stability of UO₂Cl⁺ is slightly lower than that reported in earlier publications. We note, however, that considering the uncertainty, our value for $\log \beta_1$ is in a good agreement with the values reported by Choppin and Du (1992) and Soderholm et al. (2011). The agreement with the values reported by Awasthi and Sundaresan (1980) and Davies and Monk (1957) for this formation constant, although poorer (the differences between the values are greater than the uncertainty) are still considered reasonable. In contrast to the above studies, the data reported by Ahrland (1951) and Dargent et al. (2013) suggest that the formation constant for UO₂Cl⁺ is nearly half an order of magnitude greater than that determined in our experiments (Table 3). For UO₂Cl₂° the data from the literature differ by two orders of magnitude, with log β₂ ranging from -1.2 (Awasthi and Sundaresan, 1980) to 0.74 (Dargent et al., 2013). The value obtained in our study is intermediate among the published values and is in between the values reported by Soderholm et al. (2011) and Dargent et al. (2013). The only study reporting high-temperature stability data for uranyl-chloride species is the Raman spectroscopy study of Dargent et al. (2013). Figure 10 (a,b) compares the values of the stability constants obtained in our study with those recommended by Dargent et al. (2013). Our data indicate a steady and systematic increase in the stability of uranyl-chloride species with increasing

temperature, whereas the data of Dargent et al. (2013) are more scattered and, in the case of

UO₂Cl₂°, suggest that at T≥100 °C the stability of this species is constant or even decreases with increasing temperature. The data also differ considerably in absolute terms. The values of the formation constants obtained in our study have been fitted to the Ryzhenko–Bryzgalin (MRB) model (Ryzhenko et al., 1985) modified by Shvarov and Bastrakov (1999). The latter is a model that was developed to fit the temperature and pressure dependence of dissociation constants for ion pairs:

396

397

398

399

400

401

403

404

405

406

407

408

409

410

411

412

413

414

415

416

417

402
$$\log K_{(T,P)} = \frac{T_r}{T} \log K_{(T_r,P_r)} + B_{(T,P)} \left(A_{zz/a} + \frac{B_{zz/a}}{T} \right)$$
 (13)

where K is the dissociation constant of the ion pair, T_r , P_r are the reference temperature and pressure, and $A_{zz/a}$ and $B_{zz/a}$ are fitting parameters. The term $B_{(T,P)}$ accounts for the properties of water at temperature T and pressure and P, and is computed from the data of Marshall and Franck (1981). The parameters of this model for UO₂Cl⁺ and UO₂Cl₂° are listed in Table 4. In parallel with the MRB fitting, for the above species we have also evaluated the parameters of the Helgeson-Kirkham-Flowers (HKF) model (Helgeson et al., 1981; Shock et al., 1997), which provides higher reliability for the extrapolated values. This method is described in detail in Migdisov et al. (2009). It should be noted, however, that reliable derivation of the complete set of the HKF parameters requires a large body of experimental data on the changes of the Gibbs free energy of the species of interest with both temperature and pressure. Whereas the temperature dependence can be easily calculated from the values of the formation constants (Eq. 3 and 4) using the data of Shock et al. (1997) and Johnson et al. (1992), there are no data on the pressure dependency of the Gibbs free energy of the uranyl-chloride species. In view of this, we assumed that the pressure dependence for UO₂Cl⁺ and UO₂Cl₂° is similar to that for UO₂OH⁺ and UO₂(OH)₂°, respectively, which is known (Shock et al., 1997). We therefore used the HKF parameters for the latter species reported in Shock et al.(1997) as initial guesses for our fitting (please note that in Shock et al.(1997) the stoichiometry of these species is represented as UO₂OH⁺ and UO₃(aq)°). Thus, the a₁ to a₄ HKF parameters reported in Table 5 for UO₂Cl⁺ and UO₂Cl₂°, which form part of the equation of state describing changes in the partial molar volumes of the species, are identical to those reported by Shock et al.(1997) for hydroxyl complexes of uranyl-ion. Figure 10c compares the fits performed using the MRB and the HKF models. As it can be seen from the Figure, these models return effectively identical results within the range of the experimental data obtained, however the HKF model returns more conservative values for high-T extrapolations. The above fits were used to plot diagrams illustrating the distribution of uranyl-chloride species at different temperatures as a function of the total molality of NaCl in the solutions (Figure 11a-d). The calculations were performed using the activity model of Helgeson et al. (1981), Oelkers and Helgeson (1990) and Oelkers and Helgeson (1991) for NaCl-dominated solutions (Eq.2), and accounted for ion pairing of NaCl and HCl (see description in 4.1). For comparison similar calculations were performed based on the data of Dargent et al. (2013) fitted to the MRB model (Figure 11e-h). As is evident from Figure 11, our data indicate that the uranyl ion shows very little affinity for chloride ions at low temperature and is present in the solution mostly as un-complexed UO₂²⁺ (in acidic solutions). At 25 °C, UO₂²⁺ is dominant at all concentrations of NaCl up to halitesaturation. The species distribution at 100 °C is similar to that of 25 °C, although uranyl-chloride complexes predominate at concentrations of NaCl >2m. Above 100 °C, this distribution changes dramatically. For example, at 200 °C UO₂Cl⁺ is the dominant species in solution at concentrations of NaCl as low as 0.1 m, and at 300 °C, UO₂Cl₂° is the dominant species at this and higher NaCl concentration. Our data also suggest that UO₂Cl₂° is the dominant uranyl-chloride species that will be present in common natural hydrothermal fluids (> 1 m NaCl) at all temperatures above about

418

419

420

421

422

423

424

425

426

427

428

429

430

431

432

433

434

435

436

437

438

439

250 °C. The data of Dargent et al. (2013) suggest similar behavior of uranyl species in weakly and moderately saline solutions. However, speciation diagrams plotted based on their data demonstrate higher contribution of UO₂Cl⁺ complex, and predominance of UO₂Cl₅³⁻ in solutions having concentrations greater than 1 m NaCl at T≥100 °C. We consider it likely that a major reason for the disagreement described above is the different speciation models employed in the two studies. Whereas we did not manage to identify the highly charged species, UO2Cl₄²⁻ and UO₂Cl₅³⁻, Dargent et al. (2013) assumed that these species were important contributors to the mass balance of uranyl complexes at high temperature, and, thus, fitted their spectra to models involving UO2Cl4²⁻ and UO2Cl5³⁻. As discussed earlier, an additional major reason for the disagreement is the likely inaccuracy of the activity model employed by Dargent et al. (2013) (because of their use of LiCl to supply chloride ions), especially for the spectra collected from solutions having high ionic strength; we avoided this problem by using NaCl, for which the activity model employed in the two studies was designed, and by keeping total concentrations of chloride rather low. It should also be noted that Dargent et al. (2013) observed in their experiments another species, which they were not able to identify, and which provided significant (in the case of saline solutions – the dominant) contribution to the mass balance of uranyl species in aqueous solutions. Formation of this unidentified species and its unknown stoichiometry also can significantly alter the results of their derivations. The species distribution described the potential importance of chloride ions in the transport of uranium depends enormously on temperature. At low temperature, chloride does not play a significant role in this transport, and, due to its low affinity with the uranyl ion, is an effectively inert component, contributing only to the ionic strength of the solution and the total molality. This effect has been long known from low temperature experiments and environmental studies (e.g.,

441

442

443

444

445

446

447

448

449

450

451

452

453

454

455

456

457

458

459

460

461

462

Grenthe et al., 1992; Guillaumont et al., 2003). In hydrothermal systems, however, the role of 464 chloride increases continuously and sharply with increasing temperature, and at the conditions 465 believed to be responsible for the formation of many uranium deposits (high salinity, 150-300 °C), 466 chloride complexes can effectively transport uranium. 467 Fluid inclusion data from the giant unconformity uranium deposits of the Athabasca Basin, Canada 468 (Richard et al., 2011) provide information about the fluids inferred to have been responsible for 469 ore formation. At the McArthur River deposit fluids have a salinity of up to 52 wt% (9 m) NaCl 470 equiv (Derome et al., 2005) and uranium concentrations ranging from 1.0×10^{-6} to 2.8×10^{-3} m. The 471 temperature of the fluid was estimated to have been between 120 and 200°C and the pH between 472 2.5 and 4.5. At the time of the publication of the study of Richard et al. (2011), data on uranyl-473 chloride complexation at high temperature were not available, and, in order to explain the high 474 concentrations of dissolved uranium, they assumed complete weathering of the uranium-bearing 475 minerals present in the Athabasca sandstones and the oxidation of the uranium by the fluid to UO₃. 476 The latter assumption, however, may not be valid as it is known that the sandstones contain 477 uranium as detrital uraninite, and pitchblende (e.g., Alexandre and Kyser, 2006; Risbin et al., 478 2007). Although it is possible that there was complete oxidation of the uranium present in these 479 phases, this would have required extensive interaction with surficial fluids, which seems highly 480 481 unlikely given the very high salinity of the ore fluids reported in Derome et al. (2005). On the basis of new data presented here, we suggest that a more conservative model, involving dissolution of 482 detrital uraninite and pitchblende by moderately oxidizing, saline fluids can account for the 483

We evaluated the uranyl-chloride transport model by calculating total concentrations of uranium at 200 °C in solutions of varying salinity, having a pH of 2.5, and being in equilibrium with either

formation of these ores.

484

485

pure uraninite, or pitchblende, containing 99% of uraninite and 1% of U₃O₈. The calculations were performed using our data on the stability of uranyl-chloride species (Table 4), and the data for uranyl-ion and uranyl-hydroxyl species reported by Shock et al. (1997). Other aqueous species involved in the calculations and the activity model are identical to those in the speciation model used for the treatment of our spectra (4.1). The data for uraninite and U₃O₈ were taken from Guillaumont et al. (2003). The results of these calculations are illustrated in Figure 12. The solubility of uranium shown in this figure is due mainly to uranyl-chloride complexes, except at NaCl <10 wt%, for which contributions of the uranyl ion and uranyl hydroxyl complexes is significant. Figure 12 illustrates that the saturation concentration of pure uraninite increases with salinity from 2.0×10^{-8} to 5×10^{-8} m, but is still two to five orders of magnitude lower than the concentrations determined by Richard et al. (2011). If, however, the redox potential is increased to values corresponding to the stability of pitchblende, the concentration of dissolved uranium increases by three orders of magnitude $(1.0 \times 10^{-5} \text{ to } 5 \times 10^{-5} \text{ m})$, which is well within the range of concentrations reported by Richard et al. (2011). Despite the highly simplistic nature of these calculations, they do demonstrate that chloride complexes are likely to dominate the mobilization and transport of uranium in many natural hydrothermal systems.

6.5. Conclusions

487

488

489

490

491

492

493

494

495

496

497

498

499

500

501

502

503

504

505

506

507

508

509

The data presented in this study indicate that uranyl-chloride complexes could play an important role in mobilizing uranium in natural systems and that the importance of this role will increase with increasing temperature. Although chloride has a very low affinity for the uranyl ion at ambient temperature and uranyl chloride species will not contribute significantly to the dissolution of uranium-bearing minerals and the transport of uranium in the aqueous phase at this temperature, the situation changes dramatically with increasing temperature. Between 150 and 200 °C chloride

can become one of the main ligands responsible for uranium transport in nature. Preliminary calculations performed for the fluids interpreted to have formed the McArthur River uranium deposit, Canada (Richard et al., 2011), indicate that the abnormally high concentrations of uranium in these fluids can be explained by chloride complexation of the uranyl ion. The conclusion that the role of uranyl chloride complexes in uranium transport increases with increasing temperature is in qualitative agreement with the data reported earlier by Dargent et al. (2013). We note, however, that our interpretation of the speciation disagrees strongly with that of Dargent et al. (2013), both in terms of the speciation model and the stability of the aqueous species. In contrast to the study of Dargent et al. (2013) we did not identify the highly charged species $UO_2Cl_4^{2-}$ and $UO_2Cl_5^{3-}$ in our solutions and our calculated stability constants for $UO_2Cl_2^{\circ}$ at elevated temperatures that are considerably higher than those reported in Dargent et al. (2013). Moreover, our data suggest that the species $UO_2Cl_2^{\circ}$ is the main uranyl-chloride species at $T \ge 200$ °C and chloride concentrations of relevance to naturally occurring hydrothermal solutions.

7.6. Acknowledgements

- Participation of A,T. in this study was possible due to the summer research fellowship from the
- Seaborg Institute (Los Alamos National Laboratory, USA). The authors are grateful to J-F.
- Boily, J. Brugger, and an anonymous GCA reviewer for their thoughtful and constructive
- 528 reviews.

- 530 **8.7.**References
- Ahrland S. (1951) On the complex chemistry of the uranyl ion. VI. The complexity of uranyl chloride, bromide and nitrate. *Acta. Chem. Scand* **5**, 1271–1282.
- Alexandre P. and Kyser T. K. (2006) Geochemistry of uraniferous bitumen in the Southwest Athabasca basin, Saskatchewan, Canada. *Econ. Geol.* **101**, 1605–1612.
- Anderko A. and Pitzer K. S. (1991) Equation of state for pure fluids and mixtures based on a truncated virial expansion. *AIChE J.* **37**, 1379–1391.
- Anderson G. and Crerar D. (1993) *Thermodynamics in geochemistry: The equilibrium model.*, Oxford University Press, Inc., New York Oxford.
- Awasthi S. P. and Sundaresan M. (1980) Spectrophotometric and calorimetric study of uranyl cation/chloride anion system in aqueous solution. *Indian J. Chem.*, 378–381.
- Bergstrom P.-A. and J. L. (1990) An infrared spectroscopic study of the hydration of the triflate ion (CF3SO3-) in aqueous solution. *J. Mol. Struct.* **239**, 103–111.
- Bodnar R. J. (1983) A method of calculating fluid inclusion volumes based on vapor bubble diameters and P–V–T–X properties of inclusion fluids. *Econ. Geol.* **78**, 535–542.
- Boily J.-F. and Suleimenov O. M. (2006) Extraction of Chemical Speciation and Molar
 Absorption Coefficients with Well-Posed Solutions of Beer's Law. J. Solution Chem. 35,
 917–926.
- Brugger J. (2007) BeerOz, a set of Matlab routines for the quantitative interpretation of spectrophotometric measurements of metal speciation in solution. *Comput. Geosci.* **33**, 248– 261.
- Brugger J., Liu W., Etschmann B., Mei Y., Sherman D. M. and Testemale D. (2016) A review of the coordination chemistry of hydrothermal systems, or do coordination changes make ore deposits? *Chem. Geol.* **447**, 219–259.
- Burns P. C., Ewing R. C. and Navrotsky A. (2012) Nuclear Fuel in a Reactor Accident. *Science* (80-.). 335, 1184–1188.
- Choppin G. R. and Du M. (1992) f-Element complexation in brine solutions. *Radiochim. Acta* 58/59, 101–104.
- 558 Cuney M. (2009) The extreme diversity of uranium deposits. *Miner. Depos.* 44, 3–9.
- Dargent M., Dubessy J., Truche L., Bazarkina E. F., Nguyen-Trung C. and Robert P. (2013)
- 560 Experimental study of uranyl(VI) chloride complex formation in acidic LiCl aqueous
- solutions under hydrothermal conditions (T = 21 C–350 °C, Psat) using Raman
- spectroscopy. *Eur. J. Mineral.* **25**, 765–775.
- Davies E. W. and Monk C. B. (1957) Spectrophotometric studies of electrolytic dissociation. Part 4.---Some uranyl salts in water. *Trans. Faraday Soc.* **53**, 442–449.

- Derome D., Cathelineau M., Cuney M., Fabre C., Lhomme T. and Banks D. A. (2005) Mixing of
- sodic and calcic brines and uranium deposition at McArthur River, Saskatchewan, Canada:
- a Raman and laser-induced breakdown spectroscopic study of fluid inclusions. *Econ. Geol.*
- **100**, 1529–1545.
- Dieke G. H. and Duncan A. B. F. (1949) Spectroscopic Properties of Uranium Compounds.
- National N., McGraw-Hill, New York.
- Ewing R. C. (2015) Long-term storage of spent nuclear fuel. *Nat. Mater.* 14, 252–257.
- Golub G. H. and Reinsch C. (1970) Singular value decomposition and least squares solutions.
- *Numer. Math.* **14**, 403–420.
- Greenwood N. N. and A. E. (1992) Chemistry of the Elements., Butterworth-Heinemann, Boston,
- 575 Mass.
- 576 Grenthe I., Fuger J., Konings R. J. M., Lemire R. J., Muller A. B. and Nguyen-Trung C. (1992)
- 577 CHEMICAL THERMODYNAMICS OF URANIUM. eds. H. Wanner and I. Forest, OECD
- Nuclear Energy Agency, Data Bank, Issy-les-Moulineaux (France).
- Grenthe I., Fuger J., Konings R. J. M., Lemire R. J., Muller A. B., Nguyen-Trung C. and Wanner
- H. (1992) Appendix B: Ionic strength corrections. In Chemical thermodynamics of Uranium
- (eds. H. Wanner and I. Forest). OECD-NEA, Paris. p. 717.
- Guillaumont R., Fanghänel T., Fuger J., Grenthe I., Neck V., Palmer D. A. and Rand M. H.
- 583 (2003) *Update on the chemical thermodynamics of uranium, neptunium, plutonium,*
- 584 americium and technetium.,
- Hagberg D., Karlstro G., Roos B. O. and Gagliardi L. (2005) The Coordination of Uranyl in
- Water: A Combined Quantum Chemical and Molecular Simulation Study. J. Am. Chem.
- *Soc.* **127**, 14250–14256.
- Hecht L. and Cuney M. (2000) Hydrothermal alteration of monazite in the Precambrian
- crystalline basement of the Athabasca Basin (Saskatchewan, Canada): implications for the
- formation of unconformity-related uranium deposits. *Miner. Depos.* **35**, 791–795.
- Helgeson H. C., Kirkham D. H. and Flowers G. C. (1981) Theoretical prediction of the
- thermodynamic behavior of aqueous electrolytes at high pressures and temperatures: IV.
- Calculation of activity coefficients, osmotic coefficients, and apparent molal and standard
- and relative partial molal properties to 600 °. Am. J. Sci. 281, 1249–1516.
- Hug S. J. and Sulzberger B. (1994) In situ fourier transform infrared spectroscopic evidence for
- the formation of several different surface complexes of oxalate on TiO2 in the aqueous
- 597 phase. *Langmur* **10**, 3587–3597.
- De Jagere S. and Görller-Walrand C. (1969) A Vibronic Analysis of the Absorption Spectrum of
- the Uranyl Ion. *Spectrochim. Acta* **A25**, 559.
- Johnson J. W., Oelkers E. H. and Helgeson H. C. (1992) SUPCRT92: A software package for
- calculating the standard molal thermodynamic properties of minerals, gases, aqueous

- species, and reactions from 1 to 5000 bar and 0 to 1000 °C. Comput. Geosci. 18, 899–947.
- Jones L. H. (1958) Systematics in the Vibrational Spectra of Uranyl Complexes. *Spectrochim. Acta* **10.** 395.
- Liu W., Brugger J., McPhail D. and Spiccia L. (2002) A spectrophotometric study of aqueous copper (I)-chloride complexes in LiCl solutions between 100 C and 250 C. *Geochim*. *Cosmochim*. *Acta* **66**, 3615–3633.
- Liu W., Migdisov A. and Williams-Jones A. (2012) The stability of aqueous nickel(II) chloride complexes in hydrothermal solutions: Results of UV–Visible spectroscopic experiments. *Geochim. Cosmochim. Acta* 94, 276–290.
- Marshall W. L. and Franck E. U. (1981) Ion Product of Water Substance, 0-1000°C, 1-10,000
 Bars. New International Formulation and Its Background. *J. Phys. Chem. Ref. Data* **10**, 295–304.
- Meinrath G. (1998) Aquatic Chemistry of Uranium A Review Focusing on Aspects of Environmental Chemistry. *Freib. On-line Geosci.* **1**, 0–100.
- Meinrath G. (1997) Uranium(VI) speciation by spectroscopy. *J. Radioanal. Nucl. Chem.* **224**, 119–126.
- Migdisov A. A., Reukov V. V. and Williams-Jones A. E. (2006) A spectrophotometric study of
 neodymium (III) complexation in sulfate solutions at elevated temperatures. *Geochim*.
 Cosmochim. *Acta* 70, 983–992.
- Migdisov A. A. and Williams-Jones A. E. (2006) A spectrophotometric study of erbium (III) speciation in chloride solutions at elevated temperatures. *Chem. Geol.* **234**, 17–27.
- Migdisov A. A. and Williams-Jones A. E. (2008) A spectrophotometric study of Nd(III), Sm(III)
 and Er(III) complexation in sulfate-bearing solutions at elevated temperatures. *Geochim. Cosmochim. Acta* 72, 5291–5303.
- Migdisov A. A., Williams-Jones A. E., Normand C. and Wood S. A. (2008) A
 spectrophotometric study of samarium (III) speciation in chloride solutions at elevated
 temperatures. *Geochim. Cosmochim. Acta* 72, 1611–1625.
- Migdisov A. A., Williams-Jones A. E. and Wagner T. (2009) An experimental study of the solubility and speciation of the Rare Earth Elements (III) in fluoride- and chloride-bearing aqueous solutions at temperatures up to 300°C. *Geochim. Cosmochim. Acta* **73**, 7087–7109.
- Migdisov A. A., Zezin D. and Williams-Jones a. E. (2011) An experimental study of Cobalt (II) complexation in Cl- and H2S-bearing hydrothermal solutions. *Geochim. Cosmochim. Acta* 75, 4065–4079.
- Migdisov A., Williams-Jones A. E., Brugger J. and Caporuscio F. A. (2016) Hydrothermal transport, deposition, and fractionation of the REE: Experimental data and thermodynamic calculations. *Chem. Geol.* **439**, 13–42.

- Monnin C. (1990) The influence of pressure on the activity coefficients of the solutes and on the
- solubility of minerals in the system Na-Ca-Cl-SO4-H2O to 200°C and 1 kbar and to high
- NaCl concentration. *Geochim. Cosmochim. Acta* **54**, 3265–3282.
- Nagai T., Uehara A., Fujii T. and Shirai O. (2005) Redox Equilibrium of U 4þ / U 3þ in Molten
- NaCl 2CsCl by UV Vis Spectrophotometry and Cyclic Voltammetry. J. Nucl. Sci.
- 643 *Technol.* **42**, 1025–1031.
- Nelder J. A. and Mead R. (1965) A simplex method for function minimization. *Comput. J.* 7,
- 645 308–313.
- Oelkers E. and Helgeson H. C. (1991) Calculation of activity coefficients and degrees of
- formation of neutral ion pairs in supercritical electrolyte solutions. *Geochim. Cosmochim.*
- 648 *Acta* **55**, 1235–1251.
- Oelkers E. and Helgeson H. C. (1990) Triple-ion anions and polynuclear complexing in
- supercritical electrolyte solutions. *Geochim. Cosmochim. Acta* **54**, 727–738.
- Oreskes N. and Einaudi M. T. (1992) Origin of hydrothermal fluids at Olympic Dam;
- preliminary results from fluid inclusions and stable isotopes. *Econ. Geol.* **87**, 64–90.
- Pitzer K. S. and Silvester L. F. (1978) Thermodynamics of electrolytes. 11. Properties of 3: 2, 4:
- 654 2, and other high-valence types. *J. Phys. Chem.* **82**, 1239–1242.
- Rabinovitch E. and Belford R. . (1964) Spectroscopy and Photochemistry of Uranyl
- 656 *Compounds.*, Pergamon Press, Frankfurt/Germany.
- Richard A., Rozsypal C., Mercadier J., Banks D. a., Cuney M., Boiron M.-C. and Cathelineau M.
- 658 (2011) Giant uranium deposits formed from exceptionally uranium-rich acidic brines. *Nat.*
- 659 *Geosci.* **5**, 142–146.
- Risbin D. B., Utts C. C., Uirt D. Q., Ortella P. P. and Lson R. A. O. (2007) Unconformity-
- Associated Uranium Deposits of the Athabasca. *Miner. Depos. Canada A Synth. Major*
- Depos. Dist. Metallog. Evol. Geol. Prov. Explor. Methods Geol. Assoc. Canada, 273–305.
- Ruipérez F. and Wahlgren U. (2010) Charge Transfer in Uranyl(VI) Halides [UO 2 X 4] ²⁻ (X =
- F, Cl, Br, and I). A Quantum Chemical Study of the Absorption Spectra. J. Phys. Chem. A
- 665 114, 3615–3621.
- Runde W. (2000) Spectroscopies for Environmental Studies of Actinide Species. Los Alamos
- 667 *Sci.* **26**, 412–415.
- Runde W., Neu M. P., Conradson S. D., Clark D. L., Palmer P. D., Reilly S. D., Scott B. L. and
- Tait C. D. (1996) Spectroscopic Investigation of Actinide Speciation in Concentrated
- 670 Chloride Solution. *MRS Proc.* **465**.
- Ryzhenko B. N., Bryzgalin O. V., Artamkina I. Y., Spasennykh M. Y. and Shapkin A. I. (1985)
- An electrostatic model for the electrolytic dissociation of inorganic substances dissolved in
- 673 water. *Geochem. Int.* **22**, 138–144.

- Sander R. (2006) Compilation of Henry's law constants for inorganic and organic species of
 potential importance in environmental chemistry., Air Chemistry Department, Max-Planck
 Institute of Chemistry.
- Seward T. M., Williams-Jones A. and Migdisov A. (2014) The Chemistry of Metal Transport
 and Deposition by Ore-Forming Hydrothermal Fluids. In *Treatise on Geochemistry (Second Edition)* (eds. Heinrich D. Holland and K. K. Turekian). Elsevier Ltd., Oxford. pp. 29–57.
- Shock E. L., Sassani D. C. and Betz H. (1997) Uranium in geologic fluids: Estimates of standard partial molal properties, oxidation potentials, and hydrolysis constants at high temperatures and pressures. *Geochim. Cosmochim. Acta* **61**, 4245–4266.
- Shvarov Y. V. and Bastrakov E. N. (1999) *HCh, A Software Package for Geochemical Equlibrium Modeling: User's Guide. Record 1999/25.*,
- Soderholm L., Skanthakumar S. and Wilson R. E. (2011) Structural correspondence between uranyl chloride complexes in solution and their stability constants. *J. Phys. Chem. A* **115**, 4959–67.
- Suleimenov O. M. (2004) Simple, compact, flow-through, high temperature high pressure cell for UV-Vis spectrophotometry. *Rev. Sci. Instrum.* **75**, 3363.
- Suleimenov O. M. and Seward T. M. (1997) A spectrophotometric study of hydrogen sulphide ionisation in aqueous solutions to 350°C. *Geochim. Cosmochim. Acta* **61**, 5187–5198.
- Suleimenov O. M., Seward T. M. and Hovey J. K. (2007) A Spectrophotometric Study on Uranyl
 Nitrate Complexation to 150 °C. J. Solution Chem. 36, 1093–1102.
- Sun X., Kolling D. R. J., Mazagri H., Karawan B. and Pierron C. (2015) Investigation of charge-transfer absorptions in the uranyl UO2 2+(VI) ion and related chemical reduction of UO2 2+(VI) to UO2 +(V) by UV-Vis and electron paramagnetic resonance spectroscopies.
 Inorganica Chim. Acta 435, 117-124.
- Sverjensky D., Shock E. L. and Helgeson H. C. (1997) Prediction of the thermodynamic
 properties of aqueous metal complexes to 1000 C and 5 kb. *Geochim. Cosmochim. Acta* 61,
 1359–1412.
- Tagirov B. R., Zotov A. and Akinfiev N. (1997) Experimental study of dissociation of HCl from
 350 to 500° C and from 500 to 2500 bars: Thermodynamic properties of HCl°(aq).
 Geochim. Cosmochim. Acta 61, 4267–4280.
- Tutschku J., Hennig C., Geipel G. and Bernhard G. (2004) UV-vis measurements of uranium (
 VI) and uranium (IV) in concentrated chloride solution prepared with the electrochemical cell. FZR IRC Annu. Rep., 12.
- Wood S., Palmer D., Wesolowski D. and Bénézeth P. (2002) The aqueous geochemistry of the rare earth elements and yttrium. Part XI. The solubility of Nd (OH) 3 and hydrolysis of Nd3+ from 30 to 290 C at saturated water vapor pressure with in-situ pHm measurement. In
- Water-Rock Interactions, Ore Deposits, and Environmental Geochemistry: A Tribute to
- 711 David A. Crerar (eds. R. Hellmann and S. A. Wood). pp. 229–256.

Zanonato P., Bernardo P. Di, Bismondo A., Liu G., Chen X., Rao L., R C. N., Pado V., Uniti C.
 S. and Pado V. (2004) Hydrolysis of Uranium (VI) at Variable Temperatures (10 - 85 ° C
 J. Am. Chem. Soc. 126, 5515–5522.

Table 1. The values of misfit to the recorded spectra of two models. The "low charge model" corresponds to a fit to the spectra involving UO₂²⁺, UO₂Cl₁⁺, and UO₂Cl₂°, , and the "high charge model" to a fit involving UO₂²⁺, UO₂Cl₃-, and UO₂Cl₄²⁻.

7	1	O
/	Т	O

T °C	"low charge model"	"mixed species model"	"high charge model"
150	0.7577	10.9490	4.2707
200	0.7363	20.2455	7.7317
250	0.1857	11.6775	11.2560

Table 2. Values of the logarithms of the thermodynamic formation constants derived in this study for UO_2Cl^+ and $UO_2Cl_2^\circ$, and the uncertainty associated with this derivation. log β_1 and log β_2 correspond to Reactions 3 and 4, respectively.

T °C	$\log \beta_1$	$\log \beta_2$
25	0.02 ± 0.06	0.40 ± 0.14
50	0.25 ± 0.06	0.58 ± 0.13
100	0.55 ± 0.07	0.74 ± 0.13
150	1.09 ± 0.07	1.44 ± 0.11
200	1.59 ± 0.09	2.18 ± 0.08
250	2.28 ± 0.09	3.42 ± 0.06

Table 3. Comparison of the values of the logarithms of the formation constants obtained in this study with published values.

source	$\log \beta_1$	$\log \beta_2$
this study	0.02 ± 0.06	0.40 ± 0.14
Soderholm et al. (2011)	0.16	-0.10
Dargent et al. (2013)	0.40	0.74
Choppin & Du (1992)	0.17	
Ahrland (1951)	0.38	
Davies & Monk (1956)	0.21	
Awasthi & Sundaresan (1980)	0.23	-1.2

Table 4. Parameters of the Ryzhenko-Bryzgalin model (Ryzhenko et al., 1985) modified by Shvarov and Bastrakov (1999) derived for uranyl-chloride species based on the formation constants obtained in this study.

species	$pK_{(298)}$	$A_{zz/a}$	$B_{zz/a}$
UO_2C1^+	0.017	0.792	-46.80
$UO_2Cl_2^{\circ}$	0.396	2.673	-884.56

Table 5. Parameters of the Helgeson-Kirkham-Flowers (HKF) model (Helgeson et al., 1981; Shock et al., 1997) derived for uranyl-chloride species based on the formation constants obtained in this study and the data of Shock et al. (1997) and Johnson et al. (1992).

	UO_2Cl^+	$UO_2Cl_2^{\circ}$
$\overline{\Delta G}^{\circ}_{298}$, cal	-258883	-289270
\bar{S}°_{298} , cal K ⁻¹	6.723	11.342
$a_1 \cdot 10$	4.7640	3.7801
$a_2 \cdot 10^{-2}$	3.8529	1.4512
аз	4.2318	5.1736
$a4 \cdot 10^{-4}$	-2.9382	-2.8389
<i>C</i> 1	13.2240	53.3142
$c_2 \cdot 10^{-4}$	-3.1258	-7.6490
$\omega \cdot 10^{-5}$	1.0964	-0.0300
z:	1	0

Figure captions

738

753

754

755

756

757

758

- Figure 1. A sketch illustrating the design of the high-temperature flow-through cell used for *in* situ recording of UV-visible spectra.
- Figure 2. Molar absorbance (extinction coefficients) for simple hydrated uranyl-ion (UO₂²⁺) based on the UV-visible spectra collected in this study
- Figure 3. Isothermal sets of spectra collected at 25 (a) to 250 °C (f) for solutions having the same total concentration of uranyl ions and variable concentrations of chloride ions. The lowest spectrum in each of the sets corresponds to a chloride-free solution (UO₂²⁺ in triflic acid). The figure illustrates sets of spectra collected for solutions having 7.1 mM (25 °C) of uranyl ions (molarity changes with temperature due to the changing density of the solutions).
- Figure 4. Changes in the absorbances recorded at 414 and 430 nm as a function of total concentration of NaCl. The figure illustrates the sets of spectra collected for solutions having 7.1 mM (25 °C) of uranyl ions (molarity changes with temperature due to the changing density of the solutions). Figures c) and d) illustrate this dependence on a logarithmic scale of the concentration of NaCl.
 - Figure 5. Examples of ranks of isothermal absorbance matrices calculated as a function of the tolerance (accuracy) of the recorded spectra for temperatures from 25 to 250 °C for full (a-c) and reduced (d-f) absorbance matrices (see the text). The experimental tolerance is 0.002.
 - Figure 6. An illustration of the improvement of the goodness of the fit: the states before (a) and after (b) fitting. The first step (a) uses the values of the formation constants taken from Dargent et al. (2013) as initial guesses. The illustration of the final step (b) lists the values of the optimized formation constants.

Figure 7. An example of the profile of the overall error for the second formation constant at 150 760 °C determined by changing the guesses for this constant. The minimum on this profile corresponds 761 to the value optimized for $\log \beta_2$; the horizontal line corresponds to the calculated level of the 762 763 accuracy of the spectral recording. The area of the profile below this level determines the range of 764 uncertainty associated with this determination. Figure 8. Molar absorbances for UO₂Cl⁺ (a) and UO₂Cl₂° (b) determined from spectra collected in 765 this study. 766 Figure 9. Comparison of molar absorbances at 200 °C determined for UO₂²⁺, UO₂Cl⁺, and 767 $UO_2Cl_2^{\circ}$. 768 Figure 10. Comparison of the values of formation constants determined in this study for 25 to 250 769 °C with those recommended in Dargent et al. (2013) for UO₂Cl⁺ (a, reaction 3) and UO₂Cl₂° (b, 770 reaction 4)). The fits of MRB and HKF models to the values of formation constants determined in 771 772 this study (c). Figure 11. Distribution of uranyl-chloride species as a function of the logarithm of total molality 773 of NaCl in solution calculated for 25 to 300 °C (a-d), calculated based on the data obtained in this 774 study. Distribution of uranyl-chloride species at the same conditions (e-h), calculated based on the 775 776 data reported by Dargent et al. (2013). assuming that UO₂²⁺, UO₂Cl⁺, and UO₂Cl₂° are the only aqueous species of uranium present in the 777 solution. The calculations for 25, 100, and 200 °C (a,b, and c) were performed using the MRB 778 model (Table 4), whereas those for 300 and 400 °C (d and e) were performed using the HKF model 779 (Table 5). 780

- 781 Figure 12. The solubility of uranium in NaCl-bearing solutions at 200 °C calculated assuming
- equilibrium with uraninite, UO₂ (a), and pitchblende, UO₂+U₃O₈ (b).

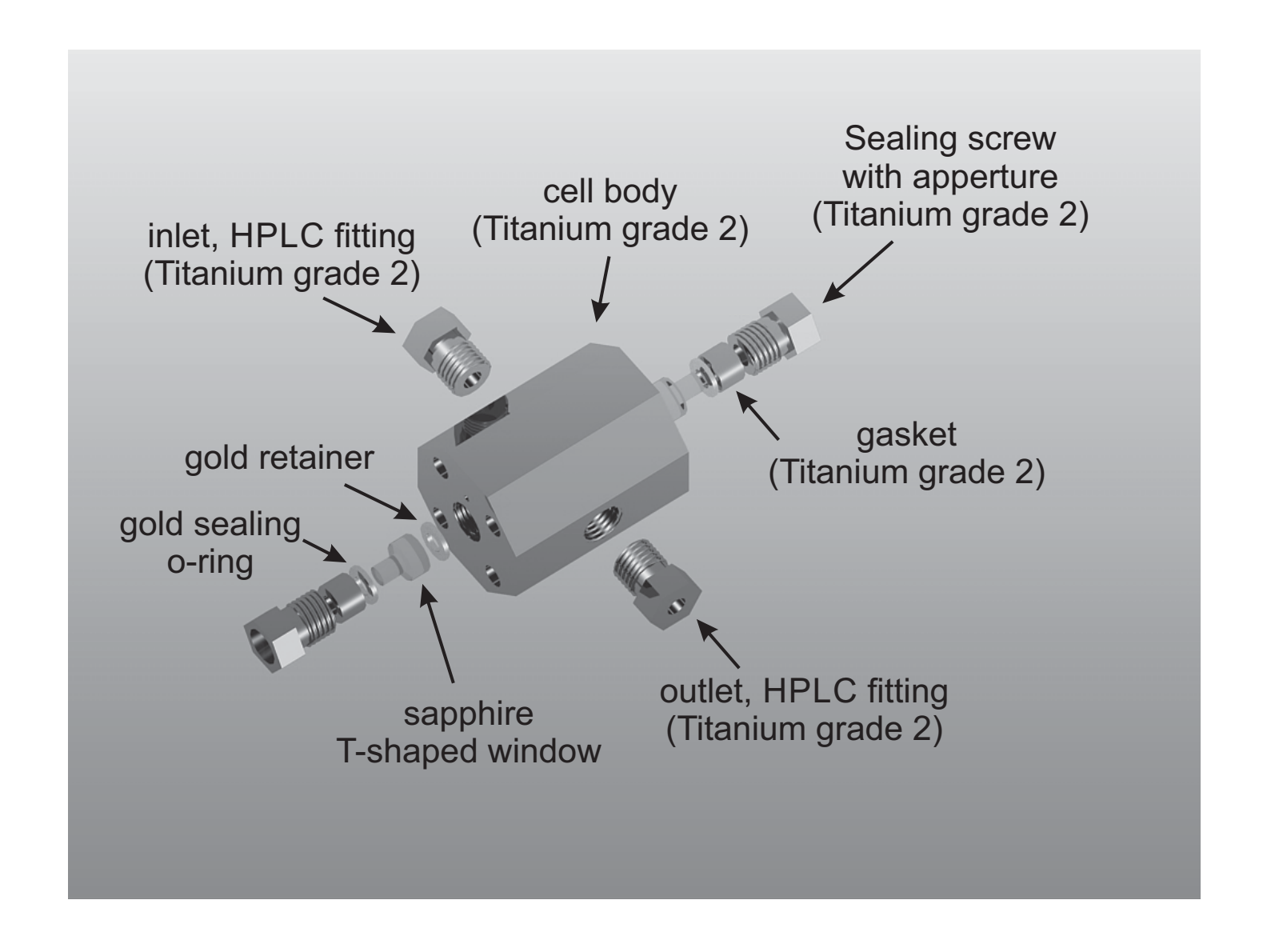


Figure 1

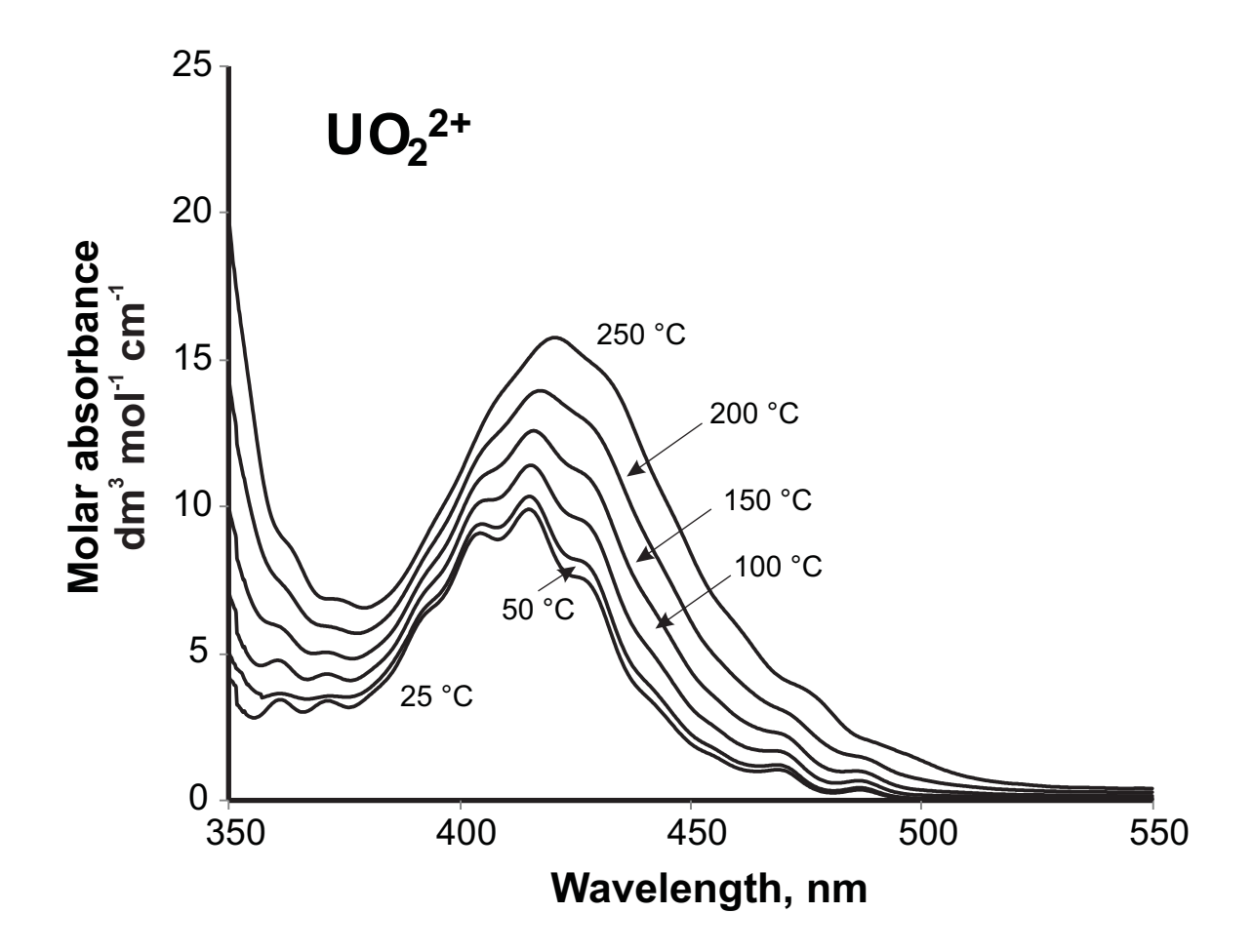
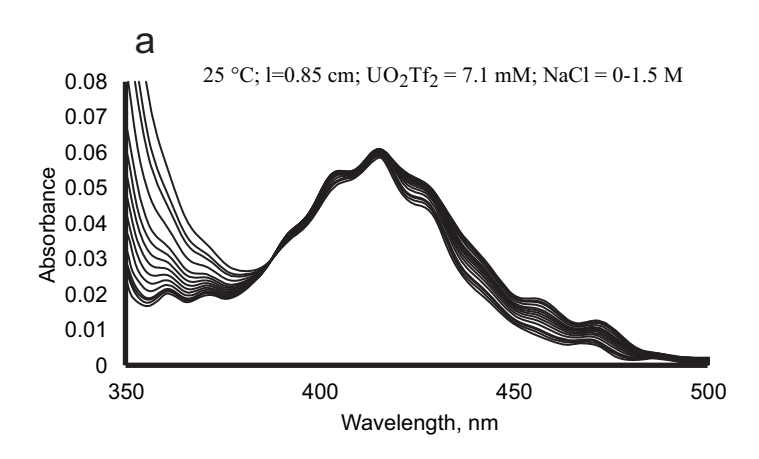
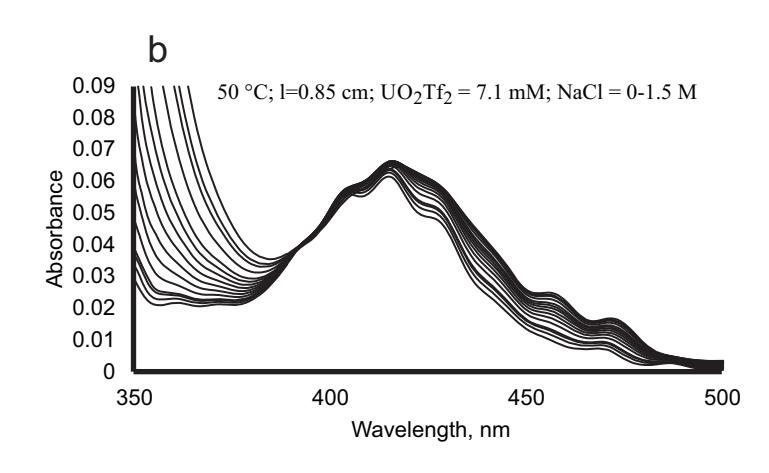
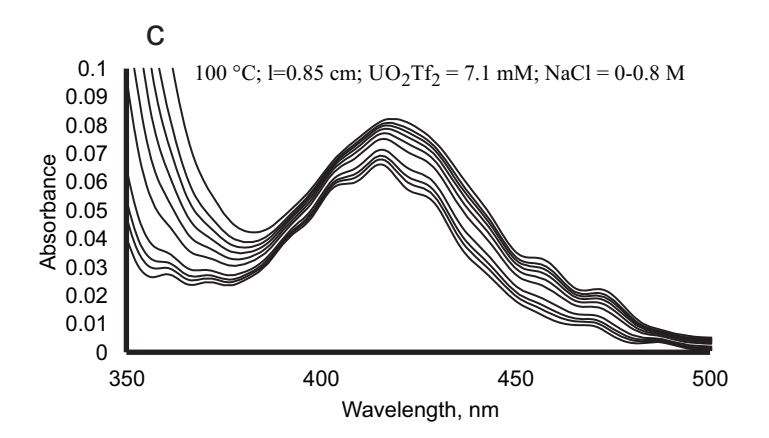
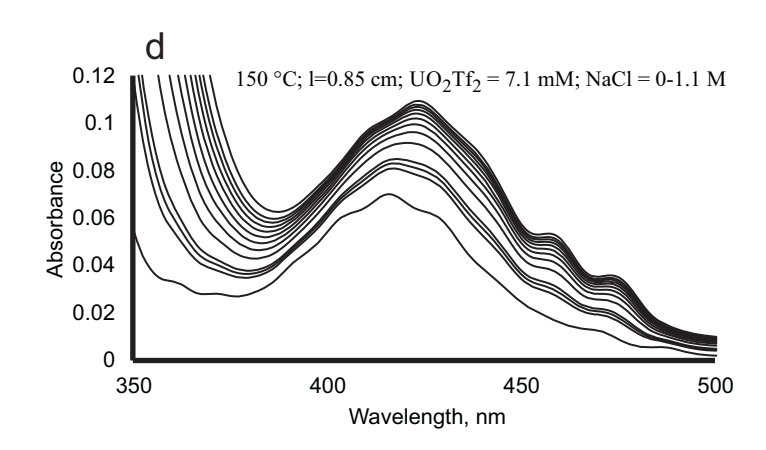


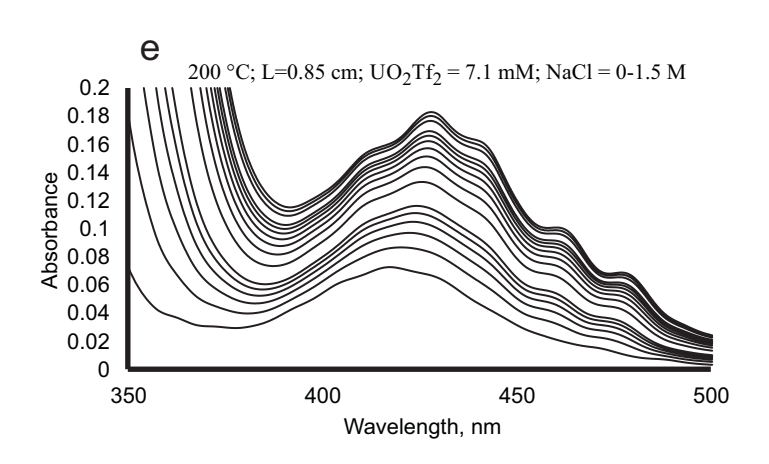
Figure 2











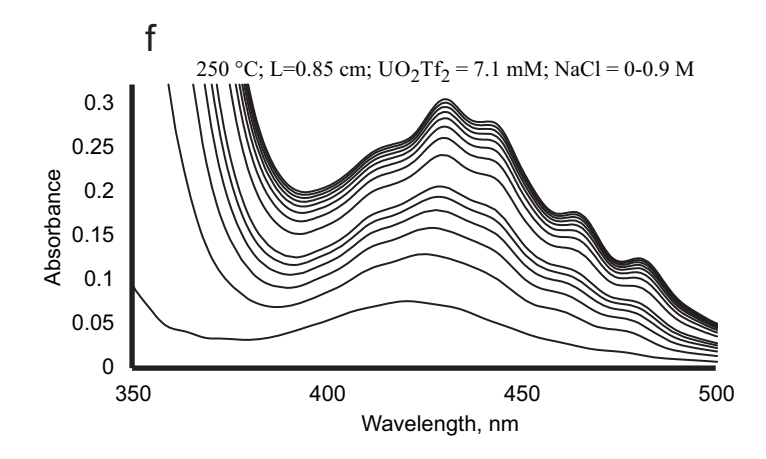


Figure 3

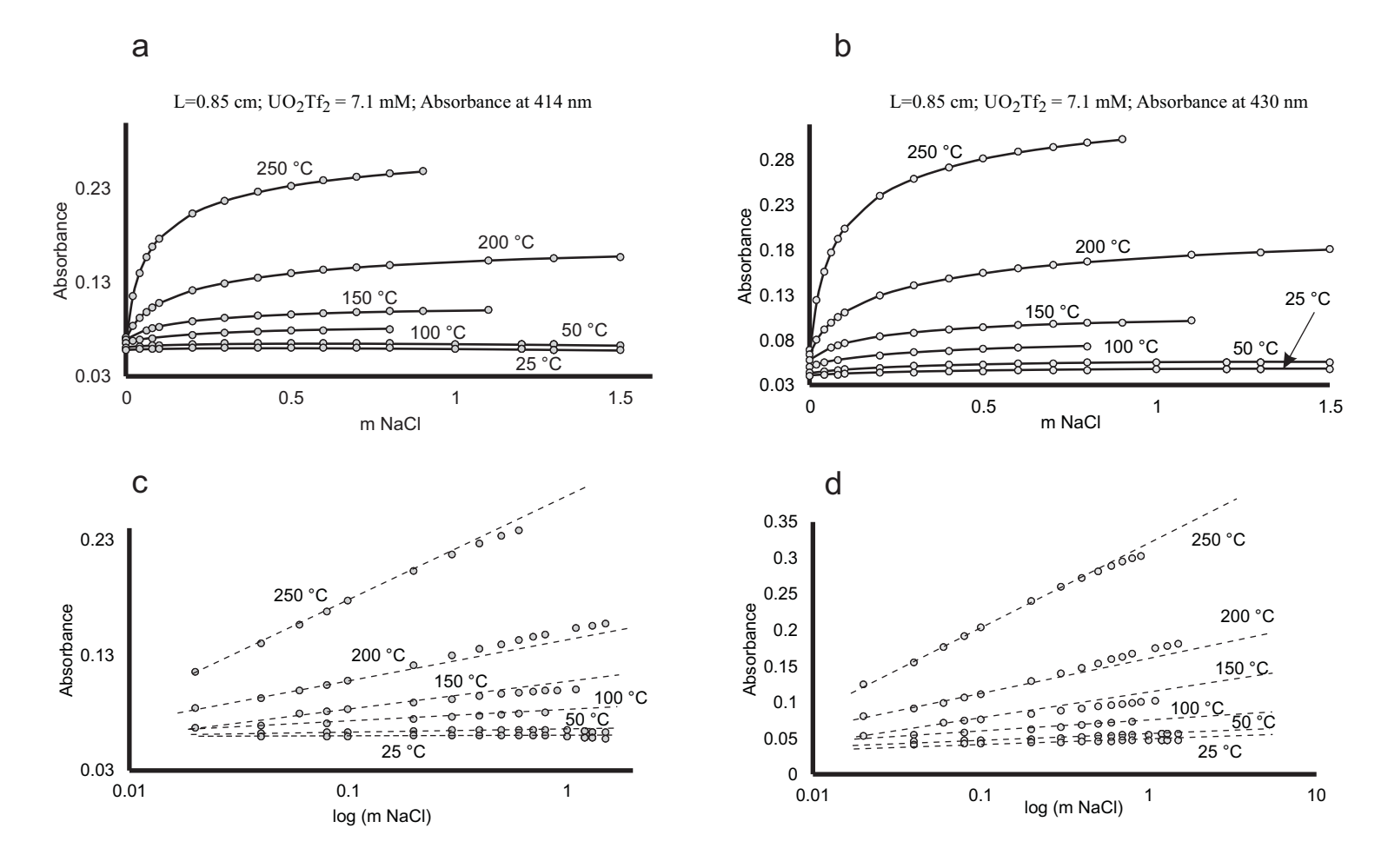


Figure 4

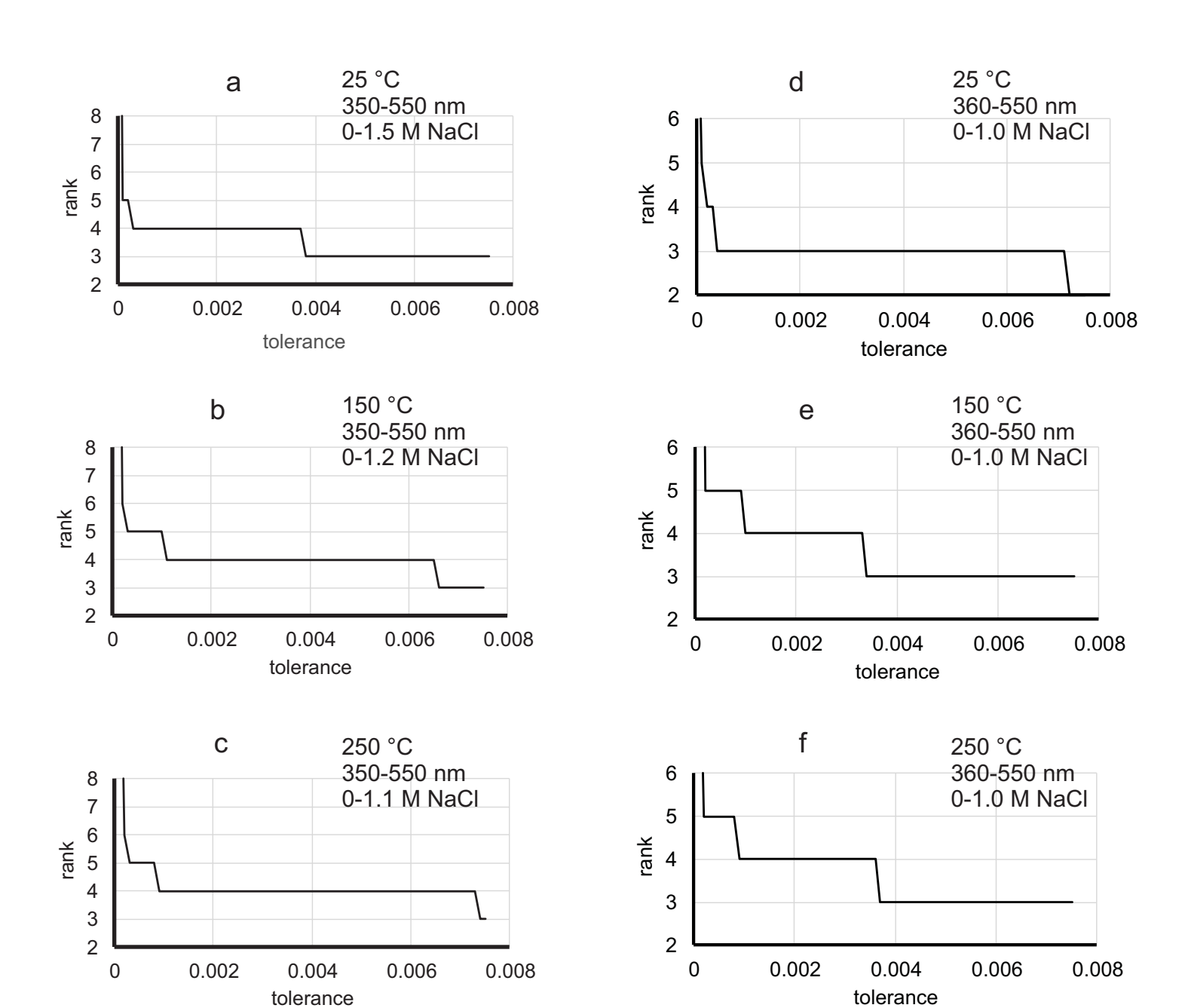


Figure 5

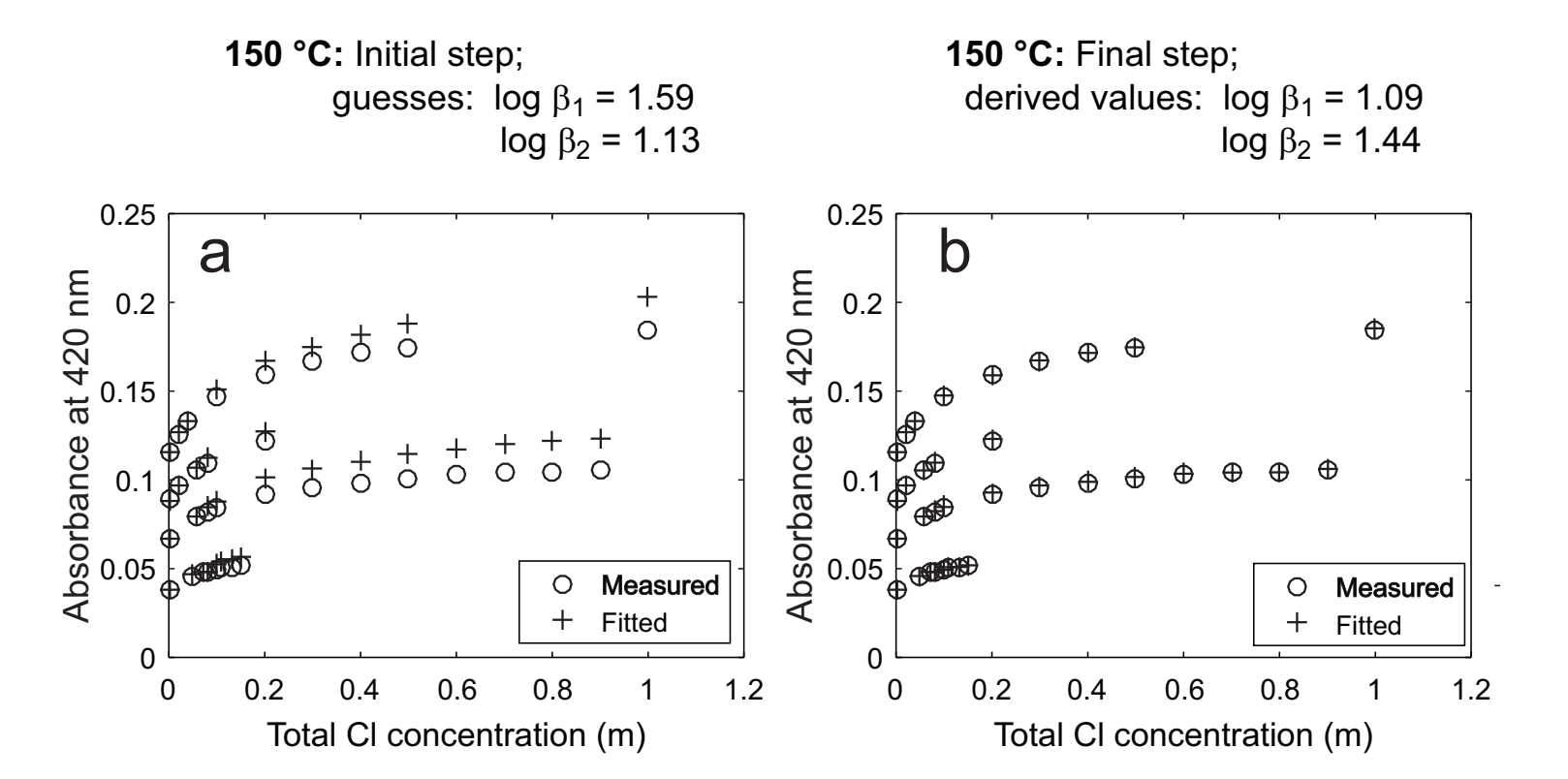


Figure 6

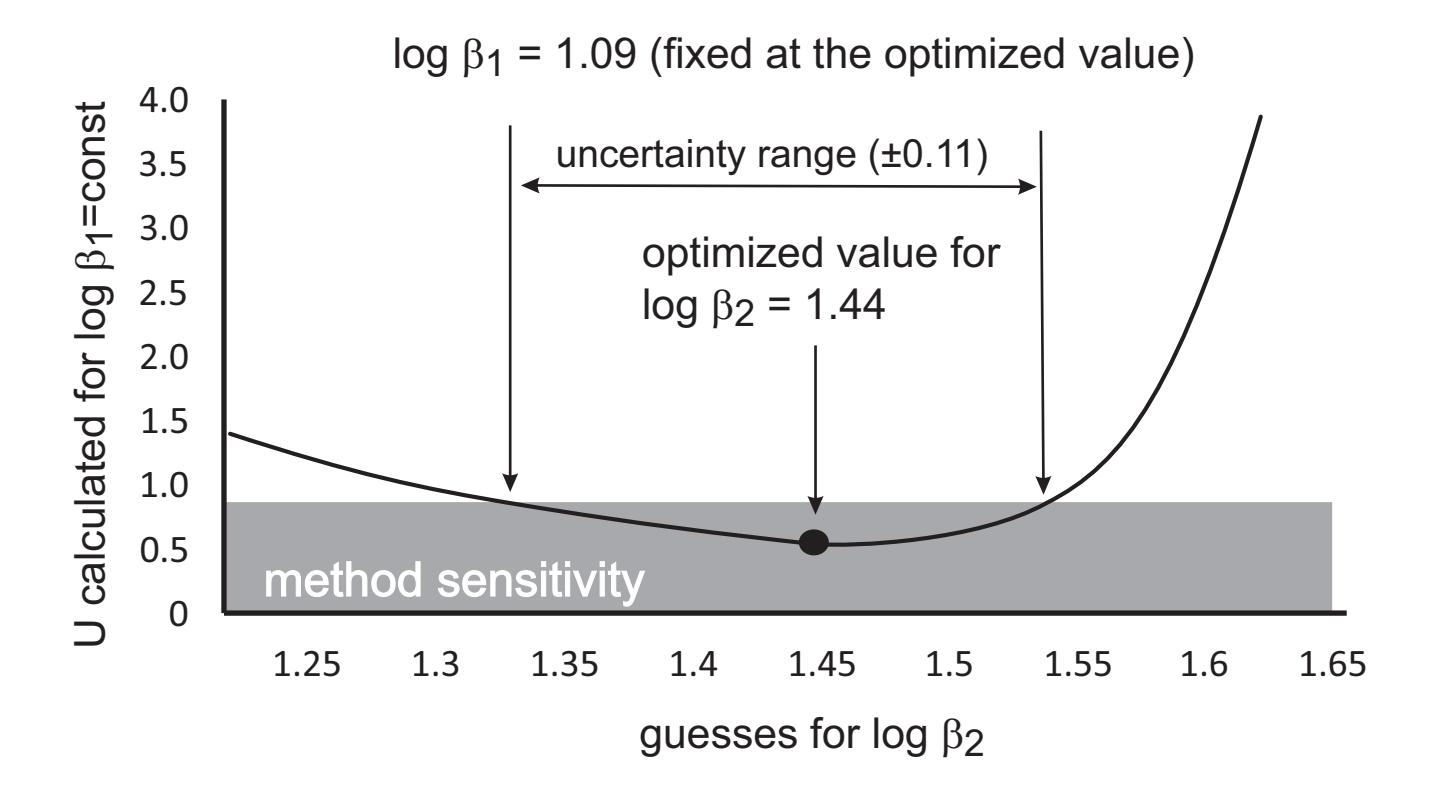
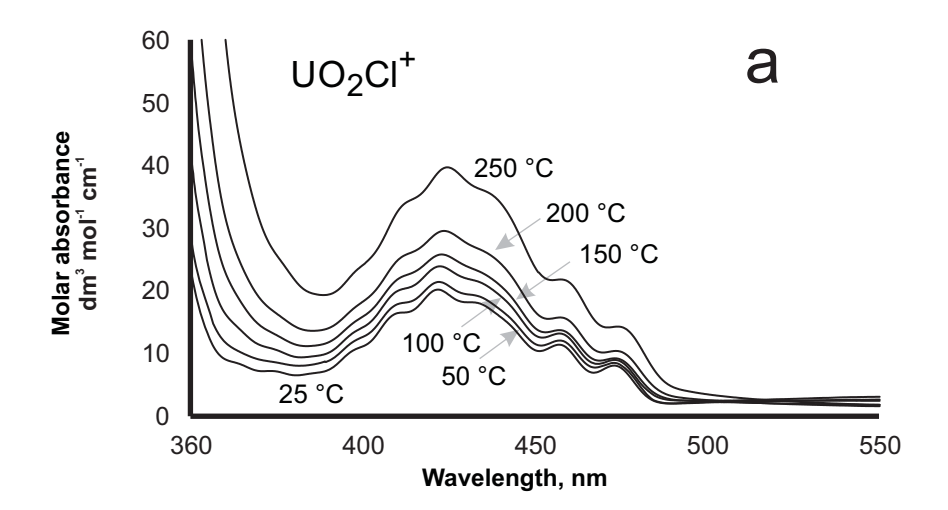
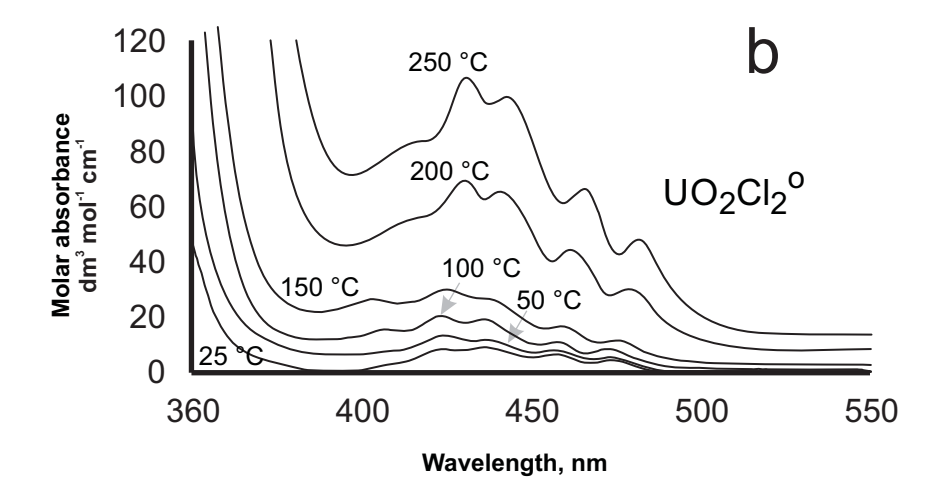


Figure 7





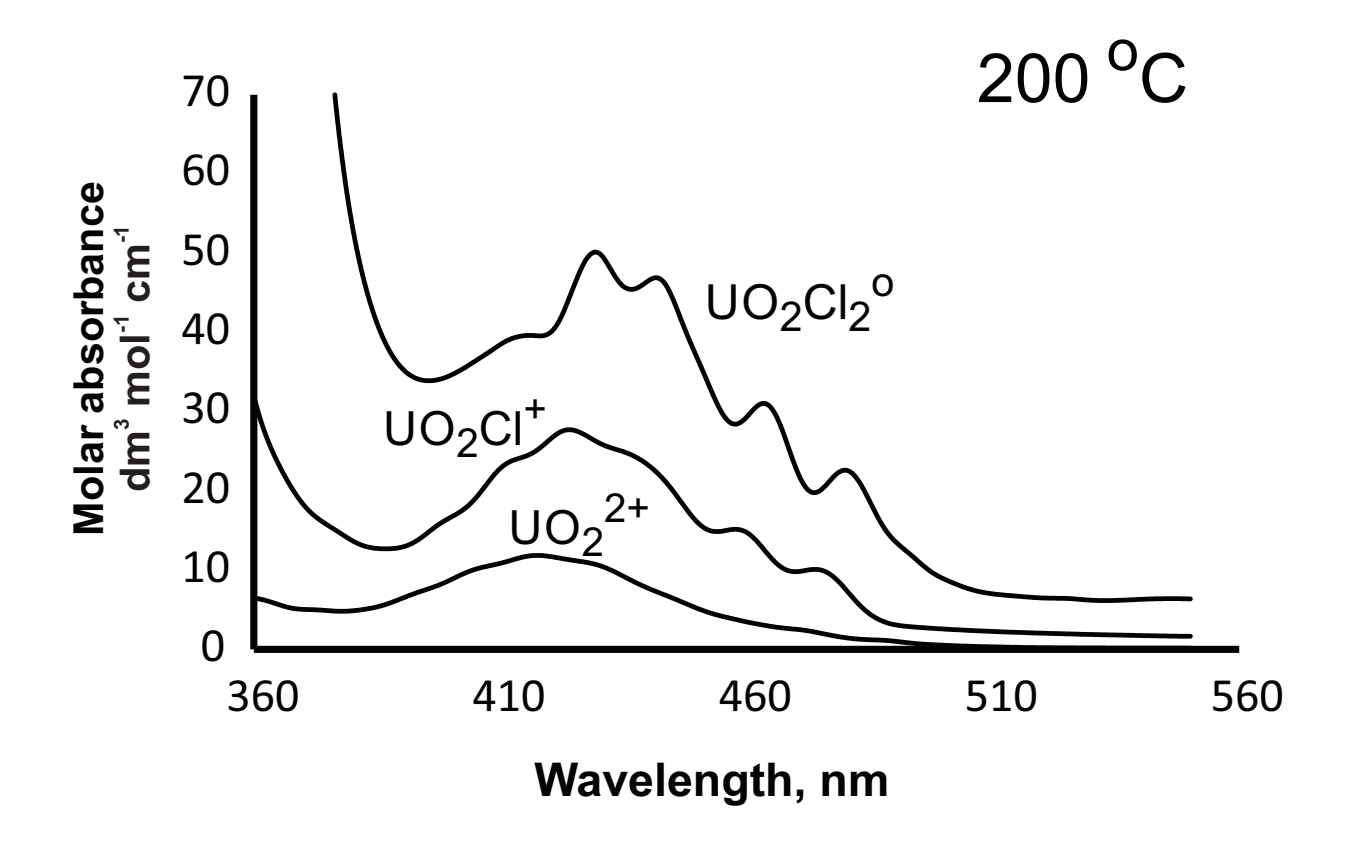


Figure 9

